

TRANSCEIVER PLATFORM FOR COMMERCIAL LTE POWER AMPLIFIERS MODELING AND LINEARIZATION

PLATAFORMA DE MODELADO Y LINEALIZACIÓN DE AMPLIFICADORES COMERCIALES CON TRANSCEPTOR RF PARA LTE

Leonardo Flores Hernández

Tecnológico Nacional de México / IT de Tijuana, México
leonardo.flores201@tectijuana.edu.mx

José Ricardo Cárdenas Valdez

Tecnológico Nacional de México / IT de Tijuana, México
jose.cardenas@tectijuana.edu.mx

Jose Alejandro Galaviz Aguilar

Tecnológico de Monterrey, México
galaviz@tec.mx

Reception: 28/october/2021

Acceptance: 20/december/2021

Abstract

In this work, a linearization scheme for QPSK and 64-QAM type digital modulation developed in an RF transceiver is presented. The modeling stage is based on a polynomial memory model with flexible memory depth and non-linearity order. In addition, an indirect learning approach (ILA) scheme is adapted for spectral correction. In this case, a sweep is performed to characterize the commercial RF power amplifier of the AD9316. Experimental results are presented to validate the QPSK with a carrier frequency of 2.4 GHz with a bandwidth of 18 MHz, and for a 64-QAM multiplexed by LTE with a bandwidth of 2.7 MHz. The improvement of the spectral growth of 8 dB for a QPSK signal of 18 MHz and it is demonstrated that it worsens by 2 dB due to the non-linear behavior of the amplifier for an LTE signal with a bandwidth of 2.7 MHz. The developed system is applicable for base stations of femtocells, picocells, and microcells. It represents the starting point of a digital predistortion (DPD) system for medium and high-power RF-PA.

Keywords: 64-QAM, LTE, QPSK, RF-PAs, transceiver.

Resumen

En este trabajo se presenta un esquema de linealización para modulación digital tipo QPSK y 64-QAM desarrollado en un transceptor de RF. La etapa de modelado se basa en un modelo polinomial de memoria con profundidad de memoria flexible y orden de no linealidad, además se adapta un esquema de enfoque de aprendizaje indirecto (ILA) para la corrección espectral. En este caso, se realiza un barrido para caracterizar el amplificador de potencia de RF comercial del AD9316. Se presentan resultados experimentales para validar el QPSK con una frecuencia portadora de 2.4 GHz con un ancho de banda de 18 MHz, y para un 64-QAM multiplexado por LTE con un ancho de banda de 2.7 MHz. Se logra la mejora del recrecimiento espectral de 8 dB para una señal QPSK de 18 MHz y se demuestra como empeora en 2 dB debido al comportamiento no lineal del amplificador para una señal LTE con un ancho de banda de 2.7 MHz. El sistema desarrollado es aplicable para estaciones base de femtocélulas, picocélulas y microcélulas y representa el punto de partida de un sistema de predistorsión digital (DPD) para RF-PA de potencia media y alta.

Palabras Clave: 64-QAM, LTE, QPSK, RF-PAs, transceptor.

1. Introduction

The continuous growth of mobile communications networks addressed to provide quality service to a long number of users lead to the challenge of developing systems that guarantee high transmission rates for voice and data [Devi, 2018], and since the radio spectrum is a finite resource, increasing bandwidth cannot be the solution to this. For this reason, digital multiplexing formats such as orthogonal frequency-division multiplexing (OFDM) require an extensive range of data to signals used in wide code division multiple access (W-CDMA), and long-term evolution (LTE), which is the standard used for broadband 5G communication networks [Franco, 2019]. Due to the demand for high bandwidth efficiency from 20 to 30 MHz [Becerra, 2020], and the need for power efficiency, the usage of the digital predistortion (DPD) techniques offers digital flexibility to linearize the undesired behavior of the power amplifiers (PAs). Since the PAs are the most critical components in an RF

transmission system, mostly given it adds most short-term and long-term memory effects during a digital information transmission, producing intermodulation products and spectral regrowth in adjacent channels [Wood, 2014]. The amplification for nonconstant envelope signals such as LTE for the power amplifier (PA) offers an optimal efficiency when operates near or beyond its 1-dB saturation point, but this tends to introduce a nonlinear distortion (NLD) on its behavior; this distortion is more significant as the ratio of peak to average power ratio (PAPR) of the input signal so that NLD will increase in 5G communication networks, [Lee, 2016]. With the rise of the Internet, billions of wireless device connections; therefore, nonlinear effects of PAs in wireless communication systems cannot be ignored [Singya, 2017]. For these reasons, interest in linearizing the behavior of amplifiers has grown lately.

Table 1 shows the estimated power output values required for 5G small and large cell applications. The 5G PAs used in femtocells and picocells have relatively low output power requirements (i.e., <20 dBm), which means it could be realized as silicon-based PAs. A macrocell for 5G needs to use GaN or GaAs PA because it requires higher output power levels. Energy efficiency, robustness, and cost will determine the appropriate device technology for a given PA 5G application [Lie, 2018].

Table 1 Power amplifier architectures associated with number of users and base stations.

Cell Type	RF P_{OUT} (dBm)	Users Number	RF P_{OUT} Per PA (dBm)	Potential PA Technologies
Femtocell	0-24	1 to 20	<20	CMOS/SOI, SiGe, GaAs
Picocell	24-30	20 to 100	<20	CMOS/SOI, SiGe, GaAs
Microcell	30-40	100 to 1000	<27	GaAs, GaN, CMOS/SOI, SiGe
Macrocell	40-47	1000+	>27	GaN, GaAs

Currently, there are many studies related to linearization and regulation of spectral regrowth applied to LTE and W-CDMA. A cubic-spline (CS) modeled with closed-loop memory involved to DPD for WCMA with a bandwidth of 5 MHz and LTE with 10 MHz is presented in [Galaviz, 2020]. The real-time DPD architecture is implemented in a commercial field-programmable gate array (FPGA), which linearizes for the 2.4 GHz band [Huang, 2020]. In the same context, some work with

parameterized Gegenbauer polynomials can be optimized for maximum efficiency and stability of the predistorter under different distributions of the input signal. The results obtained reveal exceptional numerical strength, regardless of the input signal statistics, making the proposed predistortion suitable for the linearization of broadband multimode and nonlinear wireless transmitters [Manai, 2020].

Wireless communication is everywhere in our daily life, like satellite television, navigation system, mobile phones, a global positioning system (GPS). The digital form of wireless communication is chosen over the analog form due to the various advantages, such as robustness, security, easy error detection and correction, improved performance in the communication system.

In digital transmission systems, the modulation scheme is an important part, which is classified by three aspects: amplitude shift keying (ASK), frequency shift keying (FSK), and phase shift keying (PSK). Alternatively, PSK modulation is sometimes referred to as M-ary PSK, where if $M = 2$ or 4 , then it is called binary PSK (BPSK) or quadrature PSK (QPSK), respectively. Some factors must be considered in selecting these modulation schemes, such as energy efficiency, bandwidth efficiency, low out-of-band radiation, low sensitivity to multipath fading, constant envelope. Since each of the schemes mentioned above has practical limitations and is interrelated, it is not possible to select an all-time modulation scheme that simultaneously meets all of the above factors. Mainly, the performance of QPSK is better than that of BPSK in the case of bandwidth, but it has a phase shift limitation of 180° , which destroys the constant envelope property [Noman, 2018].

The proposal in this work is to linearize MATLAB's virtual amplifier, where its nonlinear behavior is the product of selecting the Saleh model, for this the indirect learning architecture (ILA) as DPD will be used, and thus verify its usefulness with the implementation of a receive transmission with QPSK modulation through the AD9361 transceiver of an ARRadio card coupled to a SockKit card with Cyclone V FPGAs development board.

The present work involves an analysis of existing results whose main contribution is linked to reducing the spectral regrowth phenomenon; in addition to this, an implementation in a development card and the transceiver is presented as an

alternative for WCDMA-LTE applications. In Section II the traditional schemes of linearization techniques are shown, and a proposed linearization scheme based on the Indirect learning architecture (ILA) is shown. Section III shows an implementation in the frequency domain for a quadrature phase shift keying (QPSK) model. Section IV and V, the discussion and conclusions are shown respectively, and finally, in section VI, the bibliography.

2. Methods

In QPSK the carrier phase changes to the message data. The general expression to define QPSK is expressed in equation 1:

$$s_i(t) = \sqrt{\frac{2E}{T}} \cos[2\pi f_c t + \varphi_i t],, \quad 0 \leq t \leq T \quad (1)$$

Where E refers to the energy of the signal transmitted per symbol, T refers to the duration of the symbol, f_c is the carrier frequency, $\varphi_i(t)$ denotes the phase of the modulated signal for values of M and I is expressed as 1,2, ..., M, according to the equation 2.

$$\varphi_i(t) = \left(\frac{2\pi}{M}\right) (i - 1), \quad i = 1,2, \dots, M. \quad (2)$$

For QPSK modulation, the phase of the carrier signal can take four possible values in equation 3.

$$\varphi_i(t) = (2i - 1) \frac{\pi}{4},, \quad i = 1,2,3,4 \quad (3)$$

Therefore, the QPSK signal has four possible symbols; each carries two bits; these 2 bits and their corresponding signal phases are shown in table 2, [Noman, 2018].

Table 2 Signal space characteristic of QPSK.

Information of bits	Phase of QPSK signal
10	$\pi/4$
00	$3\pi/4$
01	$5\pi/4$
11	$7\pi/4$

The digital predistorter generates a nonlinear transfer characteristic that can be considered as the inverse of the transfer response of a PA in magnitude and phase, hence the PA output signal is largely counteracted by its nonlinear behavior in figure 1 shows the linearization process of a PA, wherein the DPD stage the inverse transfer response is obtained to that obtained in the PA stage (HPA), so in the end, we will obtain a linear response.

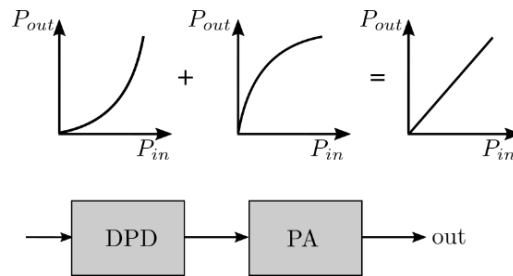


Figure 1 Block diagram for the PA linearization process with characteristics curves.

The analysis of the nonlinear behavior of a PA is feasible using different models, such as the mathematical representation utilizing a behavior model. This model requires the data measured at the input and output to obtain the necessary parameters that describe the circuit. The various modeling techniques with memory effects based on the work of Volterra are used to efficiently implement a linearization system with digital predistortion due to the precision it provides when representing nonlinear behavior and memory effects.

The Volterra series consists of a nonlinear model with memory; it is common to express the input-output relationship in terms of the complex envelopes of the signals under analysis [Wood, 2014]. The large number of coefficients that the Volterra model implies that for systems with strong nonlinearity and long memory it has encouraged for years the search for derived models where the same modeling system can be expressed with fewer coefficients. The structure of the MPM consists of several stages that introduce delays and nonlinear static functions; it is nothing more than a truncation of the general Volterra series. This only considers the diagonal terms of the Volterra kernels, thus achieving several parameters considerably less than that of the Volterra series. In this way, the MP model

introduces pairs of samples lagged for the input up to order k to describe nonlinear and memory effects [Wood, 2014]. Additionally, in [Crespo, 2019], there are alternative weighted or dynamic modeling techniques that include techniques that consider the electrical characteristics of the devices and that their calculation can be automated through iterations until the desired error is achieved.

The general equation of the MPM is defined as in equation 4.

$$y(n) = \sum_{m=0}^M \sum_{k=1}^K a_{m,k} x(n-m) [x(n-m)]^{k-1} \quad (4)$$

The coefficients that determine the behavior are obtained by the least squares method (LSM). The MPM can be subdivided into different stages, forming a block diagram, where each stage has its structure and a delay in time [Katz, 2016]. figure 2 shows the block diagram of the MPM. DPD uses digital signal processing techniques to compensate for PA-induced nonlinear distortion in wireless transmitters; DPD enables PAs to operate at high speeds in the nonlinear region and achieve high power efficiency during a transmission process. The principle of DPD is that a nonlinear function is constructed within the digital domain that is the inverse of the distortion function exhibited by the PA. In the last decades, many advanced behavior models have been proposed.

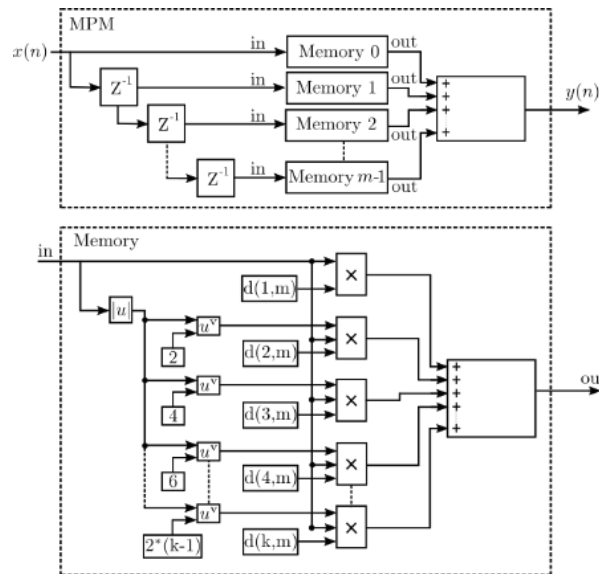


Figure 1 Block diagram for the polynomial model with memory.

If the PA is viewed as a black box, modeling the PA can generally be treated as a nonlinear system identification problem [Reina, 2015]. One might think that there should be many models available to use in DPD because the identification of the nonlinear system is very active, so there is a large field of research and where many models have already been developed over the years. In the last decades, many advanced behavior models have been proposed. If the PA is considered a black box, the RF-PA can be treated as an identification problem of a nonlinear system [Wood, 2014]; figure 3 depicts the overview of the implemented ILA.

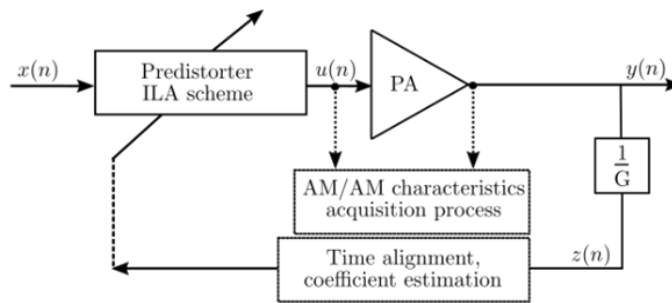


Figure 3 Indirect Learning Architecture block diagram.

The behavior modeling for derive the predistorter mode is carried out starting from the device characteristics, measurement, and modeling of an RF-PA, which considers memory effects and nonlinearity, where the function of the input and the output are interchanged as shown in equation 2, to model the nonlinear function of the DPD as is represented in equation 5. Before estimating the DPD coefficients, y_d must be normalized to the input (Equation 6).

$$y(n) = \sum_{m=0}^M \sum_{k=1}^K d_{k,m} y_d(n-m) [y_d(n-m)]^{k-1} \quad (5)$$

$$y_d(n) = \frac{y(n)}{G} \quad (6)$$

From the maximum value of $x(n)$ and $y(n)$, the value of G is calculated, using a gain ratio based on the equation 7 of the line.

$$G = \frac{y(n) \max[x(n)]}{\max[y(n)]} \quad (7)$$

Where $y(n)$ is the amplifier output, $x(n)$ the input signal, and G is the inverse gain. The result of this stage, when obtaining the inverse gain, the output signal of the PA will be linear, as in figure 1. Indirect learning architecture (ILA) is a technique in which the input signal feeds the DPD, which at first works as a buffer, then its output $u(n)$ is provided to the PA, to calculate the inverse gain $1/G$, and finally, $z(n)$ feeds the post-distorter, which has the ILA algorithm that is in charge of calculating the memory and non-linearity values. Ultimately, these values are used in the DPD, [Wood, 2014]. Simulink will send data to the ARRADIO+SOCKIT target in this implementation; see figure 4. The IIO System Object is based on the MATLAB System Objects specifications, designed to exchange data over Ethernet between an ADI Hardware System connected to an FPGA/system-on-chip (SoC) platform running ADI Linux. IIO System Object is available for both MATLAB and Simulink. IIO System Object is based on the Libiio library and allows a MATLAB or Simulink model to Stream data to and from the card, control card configuration, and monitor different card parameters. A high-level diagram showing the architecture of a system is presented in figure 5.

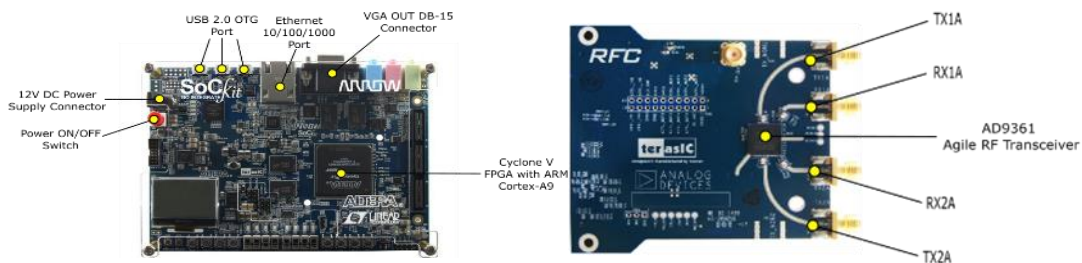


Figure 4 ARRADIO+SOCKIT Altera Cyclone V SoC-Kit.

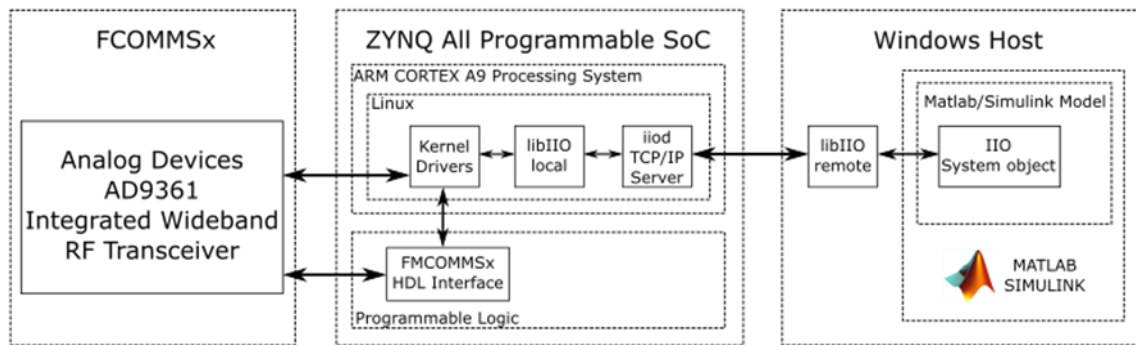


Figure 5 Top level diagram of the architecture for the system.

The input and output ports of the Simulink block corresponding to IIO System Object are used to stream data to receive/transmit full-duplex to/from the target system in a frame-based processing mode. In contrast, the control ports are used to configure and monitor different parameters of the target system. A carrier frequency of 2.4 GHz is used; on the ARRadio+Sockit target, the transmitter port TX1A is connected to the receiver port RX1A, see figure 6.

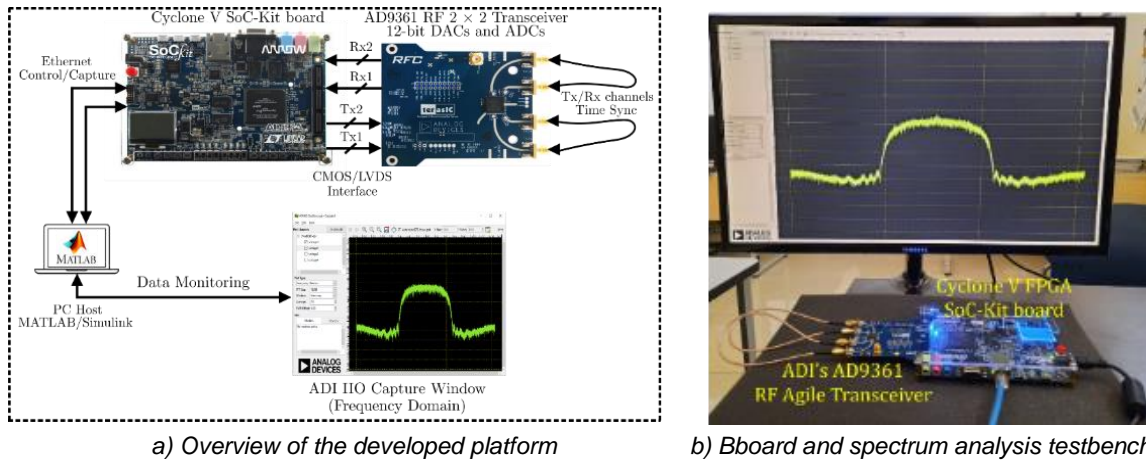


Figure 6 ARRadio+Sockit.

QPSK transmission and reception are performed; these signals are transmitted from the card to Simulink through the AD9361 block. The QPSK transmitter mainly consists of a baseband QPSK modulator, a high cosine filter, and a gain block to scale the signals before transmission. The QPSK receiver consists of the following blocks: an automatic gain control block, a receiver high cosine filter block, a coarse frequency compensation block, a refined frequency compensation block, and a time recovery block.

The amplifier block in Matlab generates a complex baseband model of an amplifier with thermal noise. When you select Saleh model for the nonlinearity modeling Method parameter, the Input scaling (dB) parameter scales the input signal before the nonlinearity is applied. The AM/AM parameters, alpha, and beta, are used to compute the amplitude gain for an input signal using the following equation 8.

$$F^{AM/AM}(u) = \frac{\alpha_1 u}{1 + \beta_1 u^2} \quad (8)$$

Where u is the magnitude of the scaled signal, the AM/PM parameters, α_1 and β_1 are used to compute the phase change for an input signal using the function depicted by equation 9. Where u is the magnitude of the input signal. Note that the AM/AM and AM/PM parameters, although similarly named α_2 and β_2 , are distinct.

$$F^{AM/PM}(u) = \frac{\alpha_2 u}{[1 + \beta_2 u^2]^2} \quad (9)$$

3. Results

In the implementation, the ADI IIO oscilloscope will be used to observe the received signal; the ADI IIO oscilloscope is a multiplatform GUI application, which supports tracing the captured data in four different modes (time domain, frequency domain, constellation, and correlation crusade). For QPSK transmission with 2.4 GHz carrier frequency, 18 MHz bandwidth, the constellation diagram generated due to the modulation detected in the receiver is shown in figure 7.

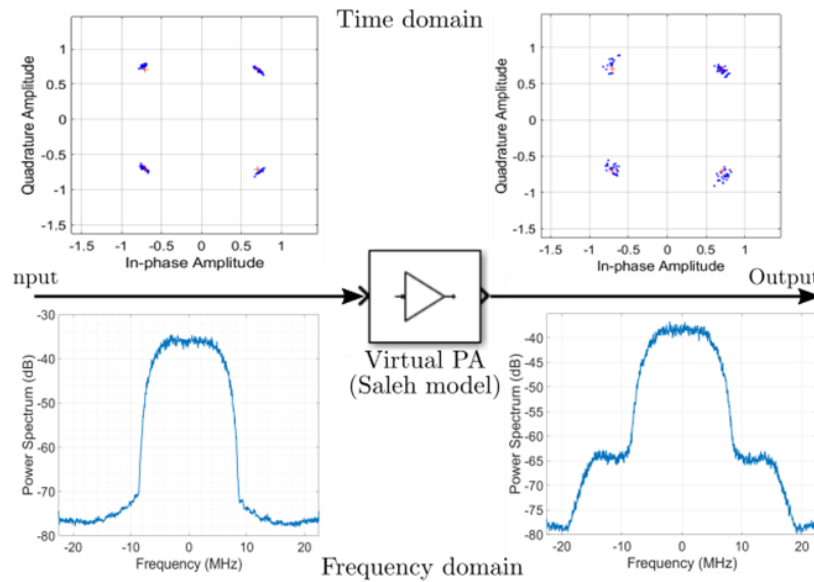


Figure 7 QPSK 18 MHz signal with EVM constellations and spectra for the input and output PA.

QPSK proposal study case

For the linearization of the MATLAB virtual amplifier (Saleh model), ILA is used in figure 7; the spectral growth of the received signal is observed as a result of the use

of the amplifier where DPD is not used as before the PA, while in figure 8 we observe the spectrum of the received signal where its power values decrease in the bands thanks to using the DPD with ILA with $m = 2$ and $k = 6$, that is, three memory stages with a depth of 6, that is, with 18 coefficients the polynomial model.

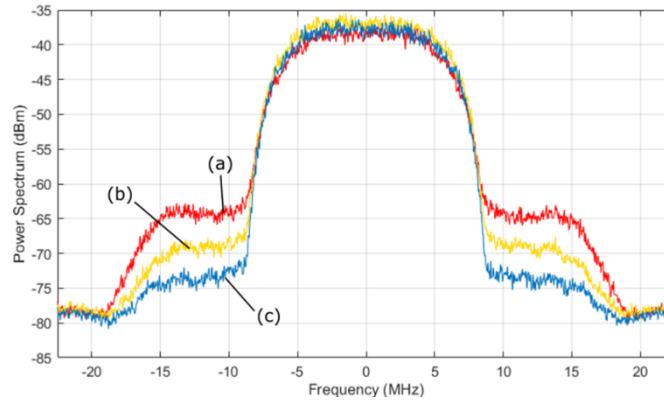


Figure 8 Spectral regrowth of the QPSK 18 MHz.

The number of coefficients determines how precise the polynomial model is; we see in table 3 the comparison of the Error Vector Magnitude (EVM), where we see that the error decreases when DPD is used to when it is not used and at the same time when the number is increased coefficients. Furthermore, the same behavior is reflected in figure 8, where when using the DPD with ILA, the power in the bands decreases, as well as when we increase the number of coefficients of the MPM.

Table 3 EVM for the QPSK signal with 18 MHz bandwidth with the two DPD cases.

Case	RMS EVM (%)	Avg EVM (dB)
Without DPD	8.4	-21.5
With DPD $k = 4$ $m = 1$	8.1	-21.9
With DPD $k = 6$ $m = 2$	7.6	-22.4

LTE proposal study case

The modeling and linearization of PAs through this method can also be applied to an LTE signal; in this case, we can model the internal amplifier that the ARRADIO+SOCKET card has, where we see in figure 9 the constellations for an LTE transmission, a signal with a 2.7 MHz bandwidth and 64 QAM modulation, where

figure 9a corresponds to the 64 QAM constellation when the amplifier works in its linear zone, and figure 9b when it works near its saturation zone, where its behavior is not linear. As expected, the error in the constellation of the symbols concerning their ideal reference increases.

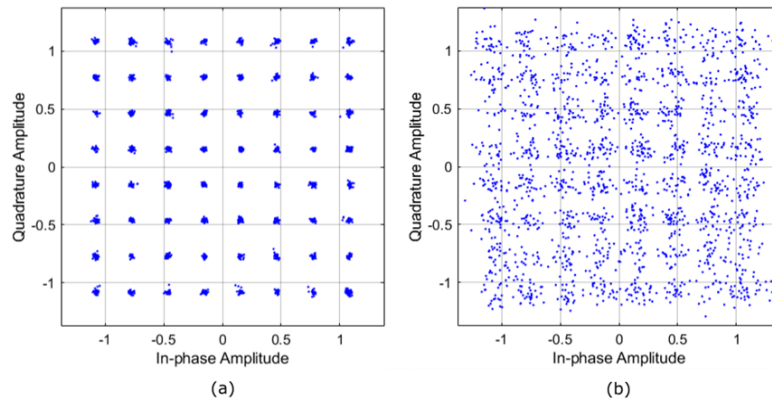


Figure 9 Constellations diagram for the input and output signal, before and after applying a scale factor.

Figure 9 shows the constellations diagram for the input and output of an LTE 2.7 MHz signal, with effects of I-Q mismatch showing amplitude and degree phase error on OFDM signal constellation before and after applying the scale factor (virtual PA is applied). Note that in figure 10, an example measures and outputs various EVM related statistics per symbol, per slot, and per frame peak EVM and RMS EVM. The example displays EVM for each slot and frame. It also displays the overall EVM averaged over the entire input waveform.

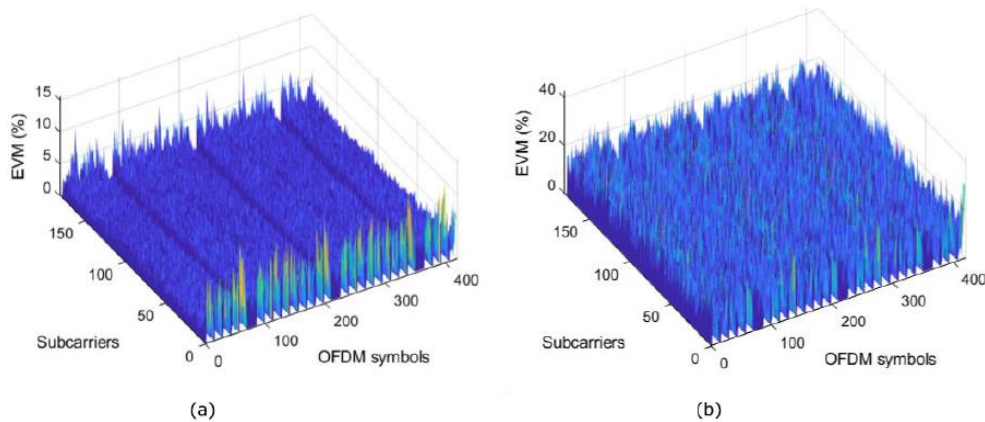


Figure 10 EVM (%) for the input and output signal, before and after applying a scale factor.

The example produces a number of plots: EVM vs per OFDM symbol, slot, subcarrier, and overall EVM. Each plot displays the peak vs RMS EVM for the channel estimation, equalization, FDD frames and subcarriers for the OFDM received waveform. In figure 10a the EVM is low near 1%, that is, the received symbols practically do not deviate from their expected position, while in figure 10b it increases considerably to almost 20 %, that is, the received symbols deviate from their expected position due to the non-linearity caused by the PA.

Figure 11 shows the spectrum of the received signal before modifying the scale factor and increasing the scale factor, bringing the amplifier of the radio AD9361 card to its saturation zone, causing spectral re-growth.

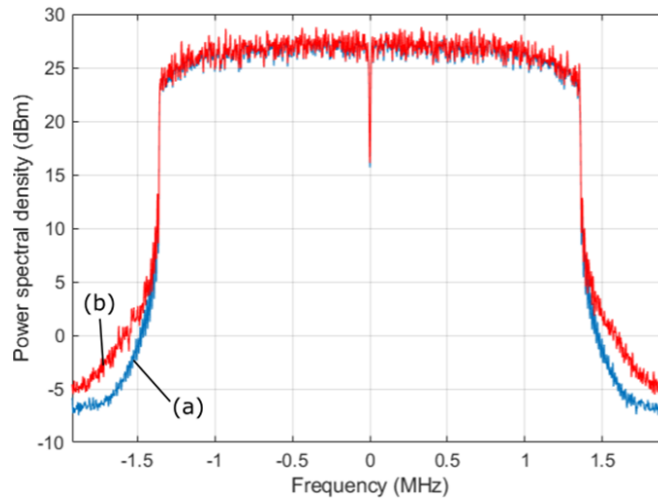


Figure 11 Baseband Signal Spectrum, (a) before and (b) after applying a scale factor.

In table 4, we observe the characteristics of the two signals transmitted in each of the 2 case studies.

Table 4 Characteristics of study cases.

Characteristics	QPSK study case	LTE study case
Modulation	QPSK	64 QAM
Sampling rate	30.72 MHz	3.84 MHz
Local Oscillator frequency	2.4 GHz	2.45 GHz
Bandwidth	18 MHz	2.7 MHz

4. Discussion

A linearization system is developed in this work associated with femtocell, picocell, and microcell applications. Current cell phone systems require modulations with high transmission speeds such as LTE and WCDMA. In this context, a complete methodology for linearizing the application of QPSK and 64-QAM is developed through this platform.

The present work represents a complete platform and methodology based on the indirect learning linearization of commercial RF-PAs with LTE applications. The methodology is based on sweeping the signal from the AD9361 dual transceiver PA for QPSK and 64-QAM modulation with 18 MHz and 2.7 MHz bandwidths. The achieved metric to evaluate the system is 8 dB of spectral reduction achieved. The developed system reaches a value of 7.5% of EVM, which is the primary specification that quantifies the performance of digital modulation. The system represents a complete platform for DPD applications based on LTE digital multiplexing schemes operating in the 2.5 GHz band.

5. Conclusions

In this paper, the indirect learning architecture is developed to linearize the nonlinear behavior of LTE commercial PAs. For this, a Simulink virtual amplifier was used as a model, where its nonlinear behavior is associated with the Saleh method; the polynomial model was used to obtain the coefficients of their behavior and thus develop the DPD with ILA, additionally is implemented for the linearization of QPSK modulation with a bandwidth of 18 MHz. An additional test was performed to test the LTE with a bandwidth of 2.8 MHz, where the amplification factor was tested in the PA. The effectiveness of this architecture to reduce the spectral growth product of the nonlinear behavior of the PA, where is verified that the number of coefficients allows improving the precision of the linear system decreasing the EVM.

EVM is evaluated for QPSK using a bandwidth of 18 MHz, and the performance is compared before and after y the ILA process. In this case, a highly nonlinear model with a nonlinearity order of 6 and memory depth of 2 was reached and 7.6 RMS EVM and -22.4 dB EVM average. An additional test was done for a reduced ILA model

using nonlinearity order of 4 and memory depth of 1 and was reached an 8.1 RMS EVM and -21.9 dB EVM average.

6. Bibliography and References

- [1] Becerra, J. A., Madero, M. J., Reina, J., & Crespo, C., Sparse Identification of Volterra Models for Power Amplifiers Without Pseudoinverse Computation. *IEEE Transactions on Microwave Theory and Techniques*, vol. 68, no. 11, noviembre, 2020.
- [2] Crespo, C., Madero, M. J., & Becerra, J. A., Volterra-based behavioral modeling, parameter estimation, and linearization. *IEEE MTT-S Latin America Microwave Conference (LAMC)*, Arequipa, Perú, Abril, 2019.
- [3] Devi, R. S., & Kurup, D. G., Behavioral modeling of RF power amplifiers for designing energy efficient wireless systems. *International Conference on Wireless Communications, Signal Processing and Networking (WiSPNET)*, Chennai, India, febrero, 2018.
- [4] Franco, I. B., Mendes, L. L., Rodrigues, J., & Cruz, M., 5G Waveforms for IoT Applications. *IEEE Communications Surveys and Tutorials*, vol. 21, no. 3, pp. 2554 – 2567, abr., 2019.
- [5] Galaviz, J. A., Vargas, C., & Tlelo, E., Automated Driving of GaN Chireix Power Amplifier for the Digital Predistortion Linearization. *IEEE Transactions on Circuits and Systems II: Express Briefs*, noviembre, 2020.
- [6] Huang, H., Xia, J., & Boumaiza, S., Novel Parallel-Processing-Based Hardware Implementation of Baseband Digital Predistorters for Linearizing Wideband 5G Transmitters. *IEEE Transactions on Microwave Theory and Techniques*, vol. 68, no. 9, septiembre, 2020.
- [7] Katz, A., Wood, J., & Chokola, D., The Evolution of PA Linearization: From Classic Feedforward and Feedback Through Analog and Digital Predistortion. *IEEE Microwave Magazine*, vol. 17, no. 2, pp. 32-40, febrero, 2016.
- [8] Lee, J., Kim, Y., Kwak, Y., Zhang, J., Papasakellariou, A., Novlan, T., Sun, C., & Li, Y., LTE-advanced in 3GPP Rel -13/14: an evolution toward 5G. *IEEE Communications Magazine*, vol. 54, no. 3, pp. 36-42, marzo, 2016.

- [9] Lie D. Y. C., Mayeda J. C., Li Y., & Lopez J., A Review of 5G Power Amplifier Design at cm-Wave and mm-Wave Frequencies. *Wireless Communications and Mobile Computing*, julio, 2018.
- [10] Manai, M., Chenini, H., Harguem, A., Boulejfen, N., & Ghannouchi, F. M., Robust digital predistorter for RF power amplifier linearization. *IET Microwaves, Antennas and Propagation*, vol. 14, no. 7, pp. 649 – 655, Junio, 2020.
- [11] Noman M. A., Ullah M. R., Hoque S., & Monirul M., Design of an improved QPSK modulation technique in wireless communication systems. *International Conference on Electrical Information and Communication Technology*, febrero, 2018.
- [12] Reina, J., Allegue, M., Crespo, C., Yu, Ch., & Cruces, S., Behavioral Modeling and Predistortion of Power Amplifiers Under Sparsity Hypothesis. *IEEE Transactions on Microwave Theory and Techniques*, vol. 63, no. 2, pp. 745-753, febrero, 2015.
- [13] Singya, P. K., Kumar, N., & Bhatia, V., Mitigating NLD for Wireless Networks: Effect of Nonlinear Power Amplifiers on Future Wireless Communication Networks. *IEEE Microwave Magazine*, vol. 18, no. 5, pp. 73-90, julio, 2017.
- [14] Wood, J., *Behavioral Modeling and Linearization of RF Power Amplifiers*. Artech House, 2014.